Experiment Title

MECH2002 – Harmonic Oscillator: Effect of Damping on Resonant Frequency

---

Team members

Emre Berna, Marcus Waterson, Nils Thiessen

Instructors

Chris Pawley, Lorenzo Reverberi, Susan du Pree

Date

08/05/2024

Introduction

The aim of this lab was to measure the effect of damping on the resonance frequency of a harmonic oscillator, thereby comparing it to what theory would dictate. A setup of two springs connected over a rotating disk, with a magnet at different distances, was built to accomplish this system.

Understanding the behaviour of harmonic oscillators proves paramount in explaining various physical concepts. Although being an ideal model, one can accurately use it to describe an object's movement around a fixed equilibrium point. This includes classical examples such as springs and pendulums, but also seismic waves or the functioning of a seismograph itself. [1] The concept plays a major role in the quantum world, where e.g. the vibrations of a diatomic molecule display a form of harmonic motion.

Theory

Harmonic oscillators can be categorized into three main types: simple, damped and driven. In a simple scenario, a mass receives an initial force, which displaces it from its equilibrium position. It will then shift back and forth around this point, and since this ideal case allows no other force to act on it, this motion will continue unhindered, characterized by the differential equation $\frac{d^2x}{dt^2} + \frac{k}{m}x = 0$. Here, m is the object's mass and k is the constant related to the restoring force.
A damped harmonic oscillator adds to the equation the loss of energy due to friction or other damping forces. One can differentiate between overdamped, critically damped and underdamped, whereby the latter will be considered in this situation. This means that depending on the object's velocity, the amplitude of oscillation, that is the farthest displacement on both ends of the equilibrium position, decreases over time. [2]
The equation thus becomes:

$$\frac{d^2x}{dt^2} + \frac{b}{m}\frac{dx}{dt} + \frac{k}{m}x = 0 \qquad (1)$$

Above, b is the damping coefficient. Finally, when applying a force $F(t)$ on the system, it is called a driven harmonic oscillator:

$$\mathrm{m}\,\frac{d^2x}{dt^2} + b\frac{dx}{dt} + kx = F(t) \qquad (2)$$

Before continuing with the theory, the setup must be briefly explained.

Fig.1: Setup for the PASCO driven damped harmonic oscillator. [3]

Two springs are connected over a rotating metal disk along a string. This system constitutes a total spring constant k. The oscillation occurs at a fixed frequency f unique to the setup. A rotary motion sensor will then be able to measure the corresponding displacement of angular nature, according to a rotating disk's moment of inertia I. With a period $P = 2\pi\sqrt{\frac{I}{k}}$, the undamped natural frequency of the undriven system is found to be:

$$\omega_0 = \sqrt{\frac{k}{I}} \qquad (3)$$

In the presence of damping, the natural frequency will decrease accordingly, the new damped natural frequency is then described as:

$$\omega_n = \omega_0\sqrt{1-\zeta^2} \quad (4)$$

$\zeta = \frac{b}{2\sqrt{kI}}$ portrays the damping ratio.
A driver arm will produce the periodic force $F(t)$ through rotation of one end of the string attached to one spring, at a distinct angular frequency ω. When this value approaches the system's natural frequency ω_n, resonance between these two "vibrations" will be caused, meaning that the amplitude of oscillation will drastically increase.
A magnet next to the metal disk will generate a magnetic drag force as the disk rotates through the perpendicular magnetic field, noticeable at higher rotation speeds. The closer the magnet, the greater the related damping coefficient b. In the absence of any driving, the differential equation can be written as $\frac{d^2\theta}{dt^2} + \frac{b}{I}\frac{d\theta}{dt} + \frac{k}{I}\theta = 0$, where the solution below accurately describes the motion. [3]

$$\theta = \theta_0 e^{-\frac{b}{2I}t}\sin(\omega t + \varphi) \qquad (5)$$

The periodic force changes the equation:

$$\mathrm{I}\frac{d^2\theta}{dt^2} + b\frac{d\theta}{dt} + k\theta = \tau_0\cos(\omega t) \qquad (6)$$

τ_0 can be seen as the driving torque, and the sinusoidal character thereof is described by the $\cos(\omega t)$ term. Solving this equation yields a function of angular displacement from equilibrium:

$$\theta = \frac{{}^{\tau_0}/_{I}}{\sqrt{(\omega_0^2-\omega^2)^2 + ({}^{b}/_{I})^2\omega^2}}\cos(\omega t - \varphi) \qquad (7)$$

Representing the phase shift between the driving force and the resulting motion, φ can be expressed as $\varphi = tan^{-1}(\frac{\omega b/_I}{\omega_0^2 - \omega^2})$. [4]

In the experiment, the magnet's distance towards the disk will be adjusted, causing higher damping effects as the two objects approach. The motion can be recorded in the absence of any driving forces, and curve fitted to a function equivalent to equation (5), which will yield a practical value for the damping coefficient b as well as the damped natural frequency ω_n. Next, the driving arm will rotate at varying frequencies, and the resulting maximum angular displacement for each will be graphed. Curve-fitting a graph akin to equation (7) and obtaining another solution for b, the two outcomes should be alike. Additionally, this allows finding a different value for ω_n. Comparing this to the theoretical one found through equation (4), one should be able to receive similar numerical results.
Furthermore, it is expected that other properties of driven harmonic oscillators should be adhered to by this system. However, the experiments are subject to several distinct errors, be it noise in the form of unaccounted for damping forces, or general systematic errors. One can therefore expect the results to deviate slightly.

Methods

The main setup was built in accordance with the PASCO Driven Damped Harmonic Oscillator manual [3]. Instead of a rotary motion sensor at the driver arm, a photogate was inserted. Preceding this, the moment of inertia I of the rotating disk had to be ascertained. The mass was determined to be $M = (0.12027 \pm 0.000005)\ kg$ with a negligible uncertainty, while the disk's radius was settled at $R = (0.0475 \pm 0.0005)\ m$. This resulted in $I = \frac{1}{2}MR^2 \approx 0.000136\ kgm^2$.

All sensors were connected to the PASCO Capstone software, such that data could be taken. The first step centred around the undamped natural frequency ω_0, which was theoretically determined using equation (3), $\omega_0 = \sqrt{\frac{k}{I}}$. This required knowledge about the torsional spring constant k of the whole system. Two methods were applied and compared for their accuracy, with precise value being used in further calculations. For both, the magnet was pulled away and no driving force was activated.

The first method involved attaching a small mass $m_1 = (0.02\ \pm 0.0005)\ kg$ above one spring and from the rotary motion sensor's data, reading off the resultant angular displacement θ. In theory, the system's restoring constant k could be calculated with $k = \frac{\tau}{\theta}$, where $\tau = r_{groove} * F = r_{groove} * mg$. Here, r_{groove} was evaluated to be $r_{groove} = (0.025 \pm 0.0005)\ m$.

Another way entailed finding the period P and plugging it into $k = \left(\frac{2\pi}{P}\right)^2 I$. As P is the system's natural time of one oscillation, it should not change under ideal circumstances. This meant that one could plot the angular displacement for multiple oscillations, yield the time difference between two distant amplitudes and divide this quantity by the number of oscillations.

An experimental value of the damped natural frequency ω_n then had to be found. The driving arm's rotation frequency depended on the voltage that was supplied to it. By slowly decreasing the voltage over the signal generator and plotting the disk's maximum angular displacement relative to the driving frequency, the peak of the resulting graph was supposed to occur when the driving frequency approached the resonant frequency. In Capstone, this implied preparing a calculation for the driving frequency ($f = \frac{1}{P}$) and smoothing it with the "smooth" function. The rotary motion sensor had a high sampling rate (50 Hz). Due to the large number of datapoints, one could use the "amplitude" function to find the maximum angular displacement for each smoothed frequency. Depending on the boundary conditions inserted, the purpose is to search for the highest value in the specified upper region, and the lowest one in the specified lower region.

The magnet was setup at three different distances from the disk: 3mm, 4mm and 6mm. This could be adjusted over the screws shown in Fig.2, and the distance was estimated with paper of the corresponding thickness. For each of these, the described resonance curves were plotted.

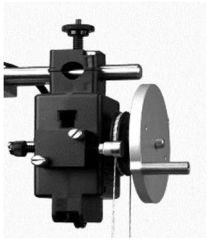

Fig.2: Magnet and metal disk. [3]

The shape of the curves can be approximated starting from equation (6). Since only the peaks for every frequency are represented (assuming the time covered a whole period for

these frequencies), the cos-term can be treated as 1. One can thus curve-fit the function $\frac{A}{\sqrt{(f^2-C^2)^2+D^2f^2}}$, where f represents the smoothed frequency. The damping coefficient b can be obtained from D.

To provide a comparison for the determined damping coefficients, the signal generator was turned off and the disk was rotated from its equilibrium position. Recording the angle versus time, one could then curve-fit a damped sine wave (like equation (4)) onto the datapoints, namely A$e^{-B}\ \sin(\omega t+\varphi)+C$. The coefficient b could then be obtained from B. A comparison on the results could then be accomplished.

The values for b then had to be examined for their similarity, and applying equation (5), the "theoretical" value for the damped natural frequency could be found.

Results & Analysis

The first method for assessing the system's spring constant k proved to be less precise. After rotating the disk to its natural equilibrium position $\theta_0 = 0\,rad$, the mass $m_1 = (0.02 \pm 0.0005)\,kg$ was first attached above the left spring, resulting in an angular displacement of $\theta_l = 1.816\,rad$. However, fixing the mass to the right spring gave $\theta_r = 1.73\,rad$. The assumption implied in the beginning had been that the spring constant measured on both sides should be the same, which appeared to not be the case. One idea was therefore to average the two spring constants $k_l = 0.0027\ \frac{Nm}{rad}$ and $k_r = 0.00284\ \frac{Nm}{rad}$, providing $k_{m1} = 0.00277\ \frac{Nm}{rad}$. However, the same procedure was repeated for a different mass $m_1 = (0.035 \pm 0.005)\,kg$. With the angular displacements $\theta_l = 3.15\,rad$ and $\theta_r = 2.86\,rad$, applying $k = \frac{\tau}{\theta}$ exhibited another value: $k_{m1} = 0.00286\ \frac{Nm}{rad}$. One can conclude from this that the strategy, as it was applied, will not yield an accurate result.

The second method centred around displacing the disk and letting it rotate freely. A plot for the disk's angle over time can be seen in Figure 3:

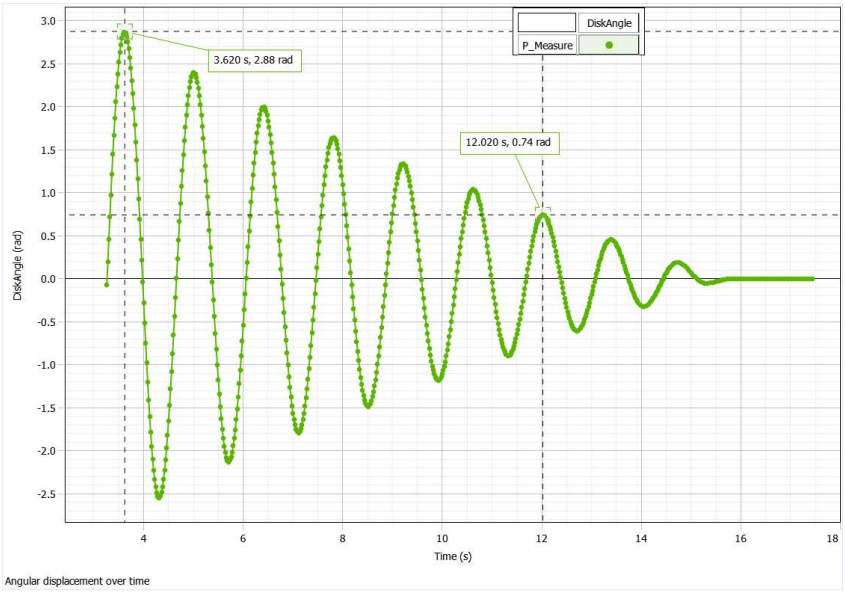

Fig.3: The system rotates freely without the magnet's or the driving arm's influence. Over time, the amplitude of oscillation decreases.

Picking two peaks 6 oscillations apart, the period was determined to be $P = \frac{\Delta t}{N_{oscillations}} = \frac{8.4\,s}{6} = 1.4\,s$. During this span, as theory suggests, the periods between consecutive peaks fluctuated minimally, with a standard deviation of $\sigma_t \approx 0.01s$. Later on, smaller frictional forces presumably affected the rotation more significantly, leading to deviating periods. Assuming σ_t as the measurement error and realizing that as Δt was a continuours recording, only the measurement of the first and last peak could have been affected by this, $\sigma_P = \frac{2}{6}\sigma_t \approx 0.00333s$ represents the error in the period. This is due to $P = \frac{\Delta t \pm 2\sigma_t}{N} = \Delta t \pm \frac{2}{6}\sigma_t$.

The spring constant then becomes: $k = \left(\frac{2\pi}{P}\right)^2 I \approx 0.0027329\ \frac{Nm}{rad}$.

Additionally, the undamped resonant frequency can be described as $\omega_0 = \sqrt{\frac{k}{I}} = \frac{2\pi}{P} \approx 4.48799\ \frac{rad}{s}$.

For each distance between magnet and disk, the angular driving frequency ω was slowly decreased and plotted against the related angular amplitude, representing the highest angular displacement of the disk due to ω. A curve-fit was implemented, where the peak of the graph depicted the experimentally derived damped resonant frequency ω_0. For the $6\ mm$ distance, this meant:

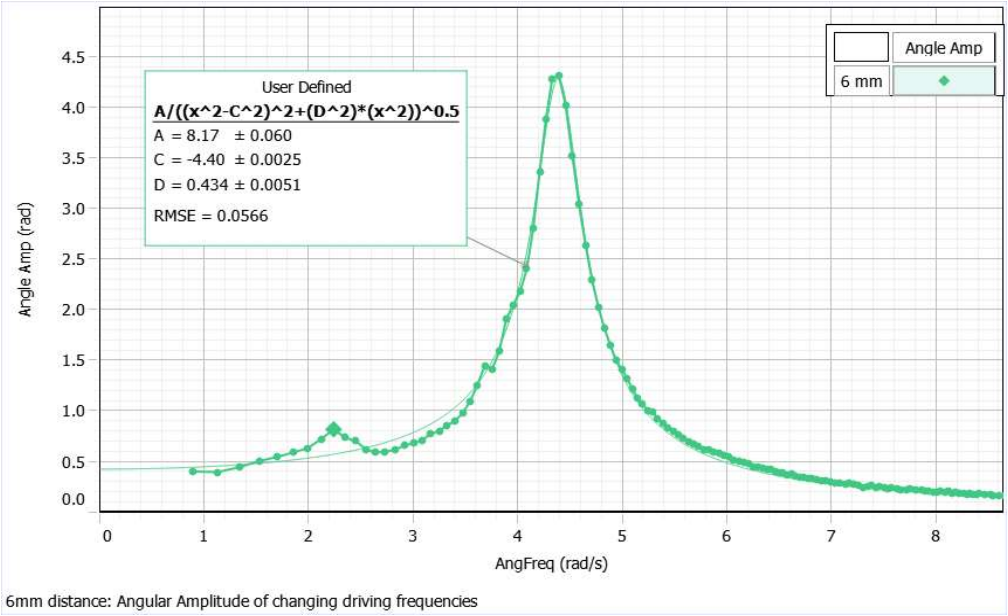

Fig.4: Resonance curve caused by a distance of 6 mm between magnet and disk. The graph spikes at the resonant frequency and has a smaller peak at half the resonant frequency.

The equation associated with the graph can be written as $\theta_6(\omega) = \frac{8.17}{\sqrt{(\omega^2-4.4^2)^2+0.434^2\omega^2}}$, with the peak at $\boldsymbol{\omega'_6 \approx 4.3893\ \frac{rad}{s}}$. This is the corresponding (experimentally acquired) damped natural frequency. A comparison to the theoretical value can be made, using $\omega_n = \omega_0\sqrt{1-\zeta^2}$. ζ depends on the damping coefficient b included in $\theta_6(\omega)$ with $D = \frac{b}{I}$, meaning that $\boldsymbol{b'_6 = DI = 0.434 * 0.12027 \approx 5.88849 * 10^{-5}\ [\frac{Nms}{rad}]}$.

Further calculations can be seen below:

$$\zeta_6 = \frac{b'_6}{2\sqrt{kI}} \approx 0.04835\ [unitless]$$

$$\boldsymbol{\omega_6 = \omega_0\sqrt{1-\zeta_6{}^2} \approx 4.48274\ \frac{rad}{s}}$$

Utilizing the percentage error, the experimental value deviates from the theoretical one by $\left(\frac{\omega'_6}{\omega_6} - 1\right) * 100 \approx 2.0844\%$.

Conducting the same procedure for smaller distances between metal disk and magnet:

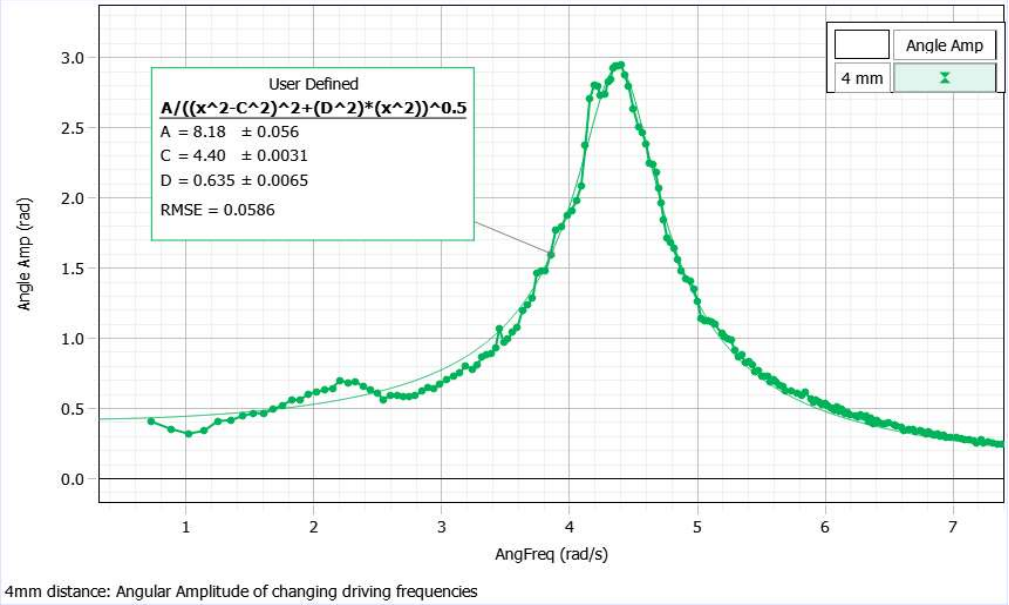

Fig.5: Resonance curve caused by a distance of 4 mm between magnet and disk. The graph spikes at the resonant frequency and has a smaller peak at half the resonant frequency.

The curve-fitted function can be expressed as $\theta_4(\omega) = \frac{8.18}{\sqrt{(\omega^2-4.4^2)^2+0.635^2\omega^2}}$, peaking at $\boldsymbol{\omega'_4 \approx 4.377\ \frac{rad}{s}}$. This implies a damping coefficient of $\boldsymbol{b'_4 \approx 8.61565 * 10^{-5}\ [\frac{Nms}{rad}]}$ and a practical damped resonant frequency of $\boldsymbol{\omega_4 \approx 4.47674\ \frac{rad}{s}}$. The deviation of the practical result from the theoretical then becomes $\left(\frac{\omega'_4}{\omega_4} - 1\right) * 100 \approx 2.2280\%$.

Lastly, for 3 mm:

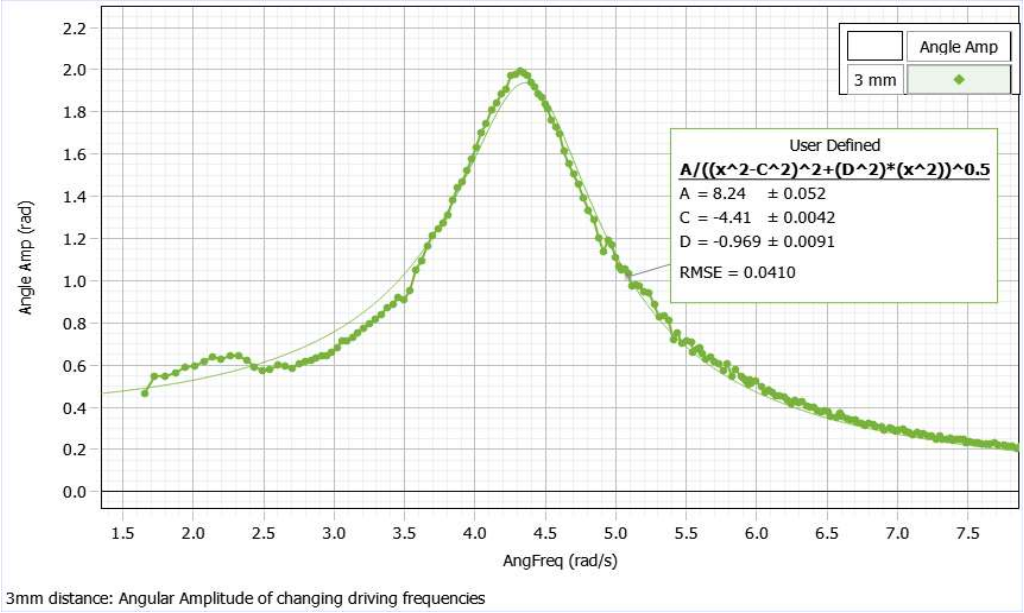

Fig.6: Resonance curve caused by a distance of 3 mm between magnet and disk. The graph spikes at the resonant frequency and has a smaller peak at half the resonant frequency.

The curve-fitted function can be expressed as $\theta_3(\omega) = \frac{8.24}{\sqrt{(\omega^2-4.41^2)^2+0.969^2\omega^2}}$, peaking at $\boldsymbol{\omega'_3 \approx 4.3564\ \frac{rad}{s}}$. This implies a damping coefficient of $\boldsymbol{b'_3 \approx 1.31474 * 10^{-4}\ [\frac{Nms}{rad}]}$ and a practical damped resonant frequency of $\boldsymbol{\omega_3 \approx 4.46176\,\frac{rad}{s}}$. The deviation of the practical result from the theoretical then becomes $\left(\frac{\omega'_3}{\omega_3} - 1\right) * 100 \approx 2.3614\%$.

For a moment of inertia $I \approx 0.000136\ kgm^2$, a spring constant of $k \approx 0.0027329\,\frac{Nm}{rad}$ and an undamped natural frequency $\omega_0 \approx 4.48799\,\frac{rad}{s}$, table 1 thus combines the results for all distances:

Distance [mm]	Damping coefficient b [10^{-5} Nms/rad]	Damping ratio ζ	Theory: Damped natural freq ω_N [rad/s]	Practice: Damped natural freq ω_N [rad/s]	Deviation [%]
6	5.88849	0.048351272	4.482740322	4.3893	- 2.0844
4	8.61565	0.070744372	4.476744749	4.377	- 2.2280
3	13.1474	0.107954798	4.461760813	4.3564	- 2.3614

Table 1: Overview data gathered from the resonance curves, along with the deviation of the practically determined ω_n from the theoretical one.

Another method of determining the damping coefficient b was proposed, meaning that if these new values would be significantly different from those of the previous method, it would potentially allow receiving a more accurate value for the damped natural frequency ω_n. For this, in the absence of the driving motor, the disk was initially rotated, released, and permitted to oscillate for a number of periods. A damped sine function, as shown in equation (5), was curve-fitted to the angle versus time datapoints. The results can be observed in Figures 7-9.

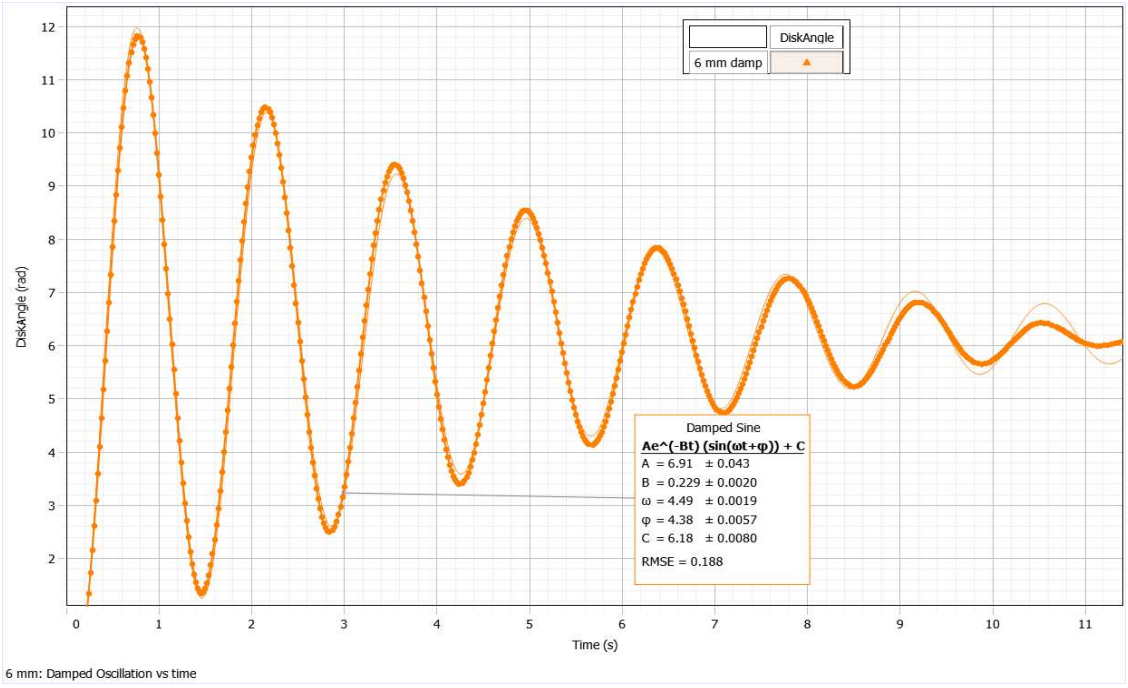

Fig.7: Damped oscillation caused by a distance of 6 mm between disk and magnet, where the disk was initially displaced by $\theta_0 \approx 6.18\, rad$. A damped sine function is curve-fitted to the graph.

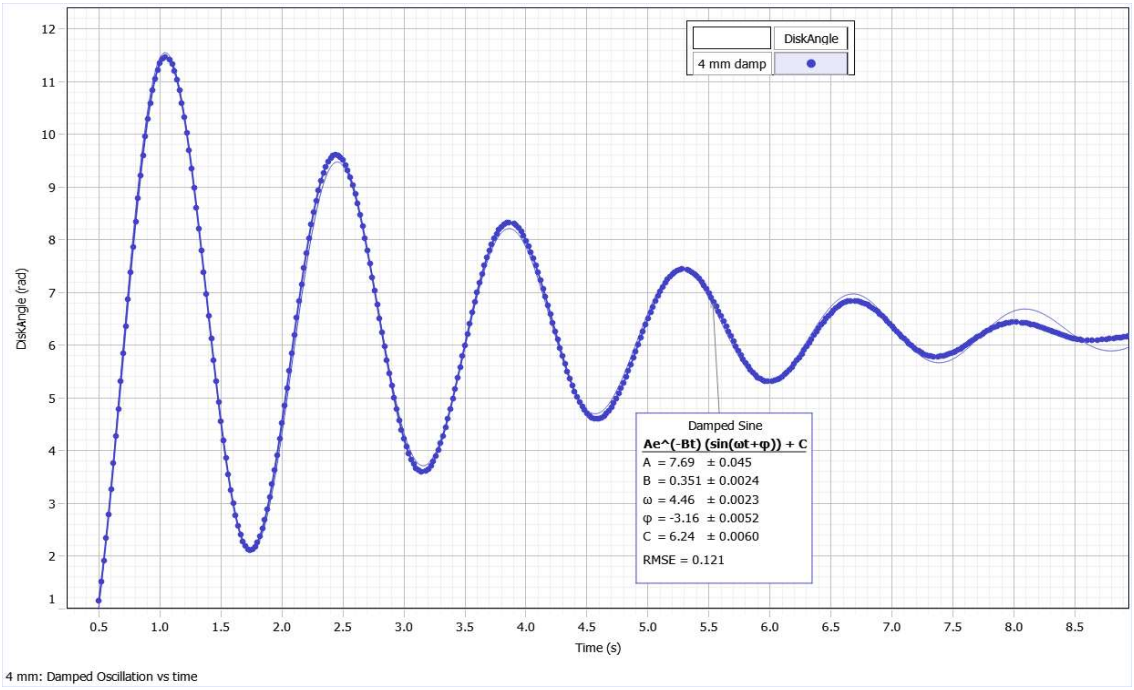

Fig.8: Damped oscillation caused by a distance of 4 mm between disk and magnet, where the disk was initially displaced by $\theta_0 \approx 6.24\ rad$. A damped sine function is curve-fitted to the graph.

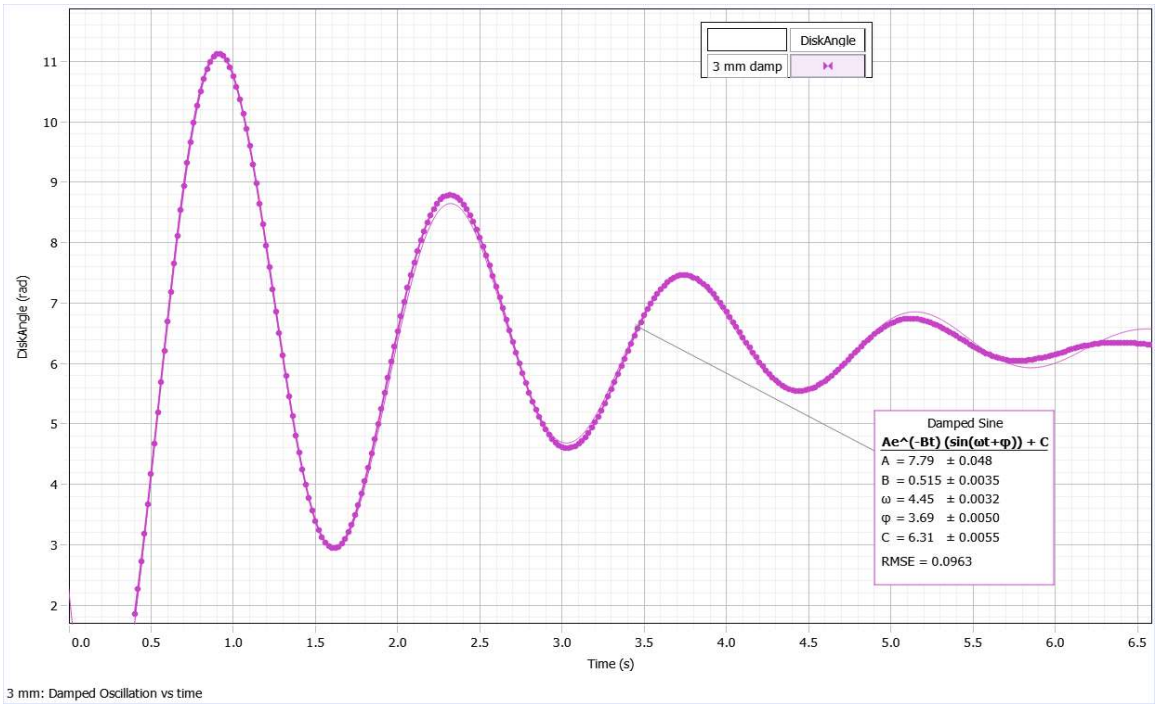

Fig.9: Damped oscillation caused by a distance of 3 mm between disk and magnet, where the disk was initially displaced by $\theta_0 \approx 6.31\ rad$. A damped sine function is curve-fitted to the graph.

The damping coefficient b is expressed in the function, with $b' = B * 2I$. From this, a table similar to Table 2 can be generated:

Distance [mm]	Damping coefficient b' [10^{-5} Nms/rad]	Damping ratio ζ	Theory: Damped resonant frequency ω_N [rad/s]	Deviation b' from b [%]
6	6.21413	0.051025075	4.482143326	5.5300
4	9.52471	0.078208739	4.474242818	10.5512
3	13.9750	0.114750714	4.45834328	6.2951

Table 2: Overview data gathered from the free oscillation curves, along with the deviation of the thereby established b' from the previous b.

The discrepancy between the damping coefficients derived from these two methods is relatively large.
The rather curious part here is that for Figures 7-9, the curve-fitted values for the angular frequency are still close to the undamped natural frequency ω_0. In fact, one can compare these "practical" values to the theoretical ones summarized in Table 2:

Theoretical Value [rad/s]	Practical value [rad/s]	Percentage error [%]
4.482143326	4.49	0.175288318
4.474242818	4.46	-0.318329134
4.45834328	4.45	-0.187138563

Table 3: Theoretical and practical value of the damped natural frequency, gathered from the free oscillation curves, as well as the deviation of the practical from the theoretical one.

For the free oscillation curves, there seems to be a higher agreement between theory and practice than for the resonance curve method. For the latter, generally speaking, the results for the damping coefficient b and the damped natural frequency ω_n deviate consistently from what is to be expected.

This implies that when activating the driving arm for the resonance curves, the undamped natural frequency is somehow affected.

Discussion

Period and spring constant

Two different strategies were utilized in finding the spring constant k. When measuring the angular displacement due to an attached mass, it became clear that the degree of rotation depended on whether the mass sat above the left or right spring. Even after averaging these two values, repeating the experiment with a different mass led to another k.
One could explain this phenomenon by the fact that the springs were tightly coiled. When stretched and compressed, they would follow Hooke's Law with the same spring constant. That is, as long if consecutive turns of the spring do not touch each other. When attaching the mass, one could assume that the tight winding caused the turns to touch, thus altering the spring constant. As the springs differed in size, there would be a decrease in resistance towards displacement between the two sides. The effect would also demonstrate why implementing a smaller mass caused a value closer to the more accurate value.
Another explanation could, obviously, be an incorrect procedure.

Finding k over the period deemed to be more precise. The period deviation was stated to be $\sigma_P \approx 0.00333s$. Due to error propagation of the formula $\omega_0 = \frac{2\pi}{P}$, the error in undamped natural frequency ω_0 thus becomes $\frac{\Delta\,\omega_0}{\omega_0} = \sqrt{(\frac{\sigma_P}{P})^2} \approx 0.00238$. Although this value is comparatively small, the new range of ω_0 now could have a drastic effect:

$$\omega_0 = (4.48799\ \pm 0.01069)\frac{rad}{s}$$

Similarly, as a result of $k = \left(\frac{2\pi}{P}\right)^2 I$, the error in the spring constant can be written as $\frac{\Delta\,\mathrm{k}}{k} = \sqrt{2 * (\frac{\sigma_P}{P})^2} \approx 0.003367$, as one can exclude the inaccuracy in I. A potential problem could arise when considering that the disk's mass density to be fluctuating throughout, but this cannot be accounted for here. The new range of k then is:

$$k = (2.7329 \pm 0.0092) * 10^{-3}\ \frac{Nm}{rad}$$

However, a rather minimal impact on the outcome of the theoretically ascertained damped natural frequencies can be ascribed here.

Ideally, either the data sampling rate or the number of surveyed oscillations should be increased. Since these approaches would narrow the errors in the period, one could achieve more accurate values for the undamped natural frequency.

Free oscillation curves

The three free oscillation curves in Figures 7-9 produce outcomes that were in line with what the theory would suggest, with the highest deviation being 0.32%. The theoretical value inherits the error of ω'_0, and together with the measurement inaccuracy of the curve-fitted, practical ω_0, the deviations can all be explained. It is worth noting that in Figures 7-9, one

can observe the fit to develop a lower precision as the angular amplitude decreases. For higher damping coefficients, this should have had a bigger effect on the curve-fit's correctness. It would be a good idea to start at a higher angular displacement, such that more oscillations could occur.

Resonance curves

On the contrary, the resonance curves diverged from the theory. The deviations in Table 1 cannot be justified by the errors alone, it appears that the procedure itself was faulty. Not only was there a high discrepancy between all damping coefficients found over both methods, but it also must be stated that the general structure of the resonance curved stayed consistent for all magnet-disk distances.
There are several explanations for this systematic problem. In contrast to the previous experiments, a force was applied over the driving arm. Although in theory, this should not affect the natural frequency at all, the state of the system could have been fundamentally altered in practice. This would mean the period, and therefore also the damped resonant frequency, could have been accurate, just for the construct with a driving arm attached. However, in the presence of a correct setup, this should not have happened.
One could also blame the PASCO Capstone functions themselves. The resonance curves heavily relied on the frequencies to be smoothed, thereby turning the continuously decreasing variable into a discrete one. To add on to that, using "amplitude" could have introduced problems itself. Nonetheless, this should have only affected the maximum amplitude for each frequency, and since the sampling rate of the rotary motion sensor (50 Hz) would normally ensure a good estimate, this does not seem to have been the cause.

In the end, another issue arises from the resonance curve. Besides the maximum amplitude, a second, smaller peak emerges at half the damped resonant frequency. The curve fit formula, which should embody the theory, does not portray this kind of behaviour. However, the fact that these peaks occur for all damping coefficients supports the idea of a systematic problem. [implication?]

Conclusion

The aim of these experiments was to measure the effect of damping on the resonant frequency. To achieve this, resonance curves (Figures 4-6) and free oscillation curves (Figures 7-9) for three different damping coefficients were plotted and curve fitted. A hypothesis was stated that the practically determined values for the damped resonant frequency would align with the theoretical ones found through equation (4), $\omega_n = \omega_0\sqrt{1-\zeta^2}$.
With the purpose of yielding a value for the spring constant and undamped resonant frequency, two methods were compared. For one of them, the angular displacement due to a mass was assessed, with inconsistent outcomes depending on the mass or where it was attached. Further research could be conducted in finding the problem's source. An idea would be to include identical springs with a less tight wiring, hopefully providing a similar number.

The second method was more precise, with $\omega_0 = (4.48799 \pm 0.01069)\frac{rad}{s}$ and $k = (2.7329 \pm 0.0092) * 10^{-3}\ \frac{Nm}{rad}$.

While for the free oscillation curves, the theoretical and practical ω_n were in compliance and thus validified the hypothesis, the resonance curves implied strong deviations. The same applied for the damping coefficient b, showing that the resonance curve method did not work as supposed to. It is therefore important to repeat the corresponding measurement, so that the cause for the discrepancies can be found.
One can do so by checking for the same magnet-disk distance twice and analysing if the results are consistent with each other, thereby demonstrating that the result is not by chance. Generally, it has to be researched what causes the effect of the driving arm on the resonant frequency, which could then be prevented in further experiments. The resonance curves also portray the maximum angular amplitude through their peaks, which can be validated through the theory.

References

[1] Mayrhofer, D. (2018). *An Exploration of the Seismograph*. https://writing.rochester.edu/celebrating/2019/David_Mayrhofer.pdf

[2] openstax. (2016). *Simple Harmonic Motion - University Physics Volume 1 - OpenStax*. Openstax.org. https://openstax.org/books/university-physics-volume-1/pages/15-1-simple-harmonic-motion

[3] Hanks, A. (n.d.). *Driven Damped Harmonic Oscillations Experiment Manual*. PASCO Scientific. Retrieved May 15, 2024, Accessed from https://www.pasco.com/products/complete-experiments/rotation/ex-5522#experiment-panel

[4] Lab coordinators et al., "MECH202 – Damped driven harmonic oscillator", 2024, Accessed from Canvas.